Systematic study of the superconducting critical temperature in two- and three-dimensional tight-binding models: A possible scenario for superconducting H_3S

Thiago X. R. Souza[1,2] and F. Marsiglio[1]
[1]*Department of Physics, University of Alberta, Edmonton, Alberta, Canada, T6G 2E1*
[2]*Departamento de Fisica, Universidade Federal de Sergipe, 49100-000 Sao Cristovao, Sergipe, Brazil*
(Received 1 June 2016; revised manuscript received 28 July 2016; published 21 November 2016)

Ever since BCS theory was first formulated it was recognized that a large electronic density of states at the Fermi level was beneficial to enhancing T_c. The A15 compounds and the high temperature cuprate materials both have had an enormous amount of effort devoted to studying the possibility that such peaks play an important role in the high critical temperatures existing in these compounds. Here we provide a systematic study of the effect of these peaks on the superconducting transition temperature for a variety of tight-binding models of simple structures, both in two and three dimensions. In three dimensions large enhancements in T_c can occur, due to van Hove singularities *that result in divergences in the density of states*. Furthermore, even in more realistic structures, where the van Hove singularity disappears, large enhancements in T_c continue due to the presence of "robust" peaks in the densities of states. Such a peak, recently identified in the bcc structure of H_3S, is likely the result of such a van Hove singularity. In certain regimes, anomalies in the isotope coefficient are also expected.

DOI: 10.1103/PhysRevB.94.184509

I. INTRODUCTION

The weak coupling Bardeen-Cooper-Schrieffer (BCS) [1] expression for the superconducting transition temperature T_c is

$$T_c \sim \omega_D e^{-1/[g(\epsilon_F)V]} \tag{1}$$

(we set $\hbar = k_B = 1$) where ω_D is the typical (Debye) phonon frequency, V is the attractive interaction strength, and $g(\epsilon_F)$ is the electron density of states at the Fermi level. This simple expression makes clear that a high value of the density of states at the Fermi energy is desirable for high T_c, and has served to motivate a directed search for high T_c materials for more than half a century. Some understanding of the impact on T_c has come historically from a study of the A15 compounds, where experiments suggested that various "anomalous" superconducting properties in these compounds could be explained by peaks (or in some cases valleys) in the electron density of states near the Fermi level.

Indeed, as early as 1967 Labbé *et al.* [2] suggested that sharp peaks in the electronic density of states could explain the high T_c and low isotope effects in some A15 compounds. They adopted a density of states with a square-root singularity, reminiscent of the result obtained in one dimension. Since that time, Nettel and Thomas [3] and Horsch and Rietschel [4] developed this model further in the context of Eliashberg theory, again with an eye towards explaining the high critical temperatures of some of the A15 compounds. Follow-up work by Lie and Carbotte [5], Ho *et al.* [6], Pickett [7], and Mitrović and Carbotte [8] served to establish the importance of peaked structures in the electronic density of states near the Fermi level for the critical temperatures in the A15 superconductors [9].

In the mid 1980s the possibility of enhancing the superconducting critical temperature through a two-dimensional structure was advanced by Hirsch and Scalapino [10], and these authors also used Monte Carlo simulations and high-order perturbation corrections to support their claims. They found enhanced superconductivity when the Fermi level was near a singularity, particularly in the weak coupling regime. These ideas were further developed with the discovery of high temperature superconductivity in 1986, and several papers [11,12] subsequently explored some of the consequences of a two-dimensional van Hove singularity for superconductivity. Rather than recount a detailed history of the various calculations, we refer the reader to review papers, a comprehensive one in 1997 [13], and a more recent review [14] focused on the A15 compounds. While the early work focused on a square-root singularity, most of the work in the past 30 years has almost exclusively utilized a density of states with a logarithmic divergence, motivated by the two-dimensional tight-binding model. A notable exception is the extended saddle point singularity pointed out through density functional theory calculations in 1991 [15] and observed through ARPES measurements and modeled in 1993 [16]. The extended saddle point results in a one-dimensional-like square-root singularity in the electronic density of states.

The theoretical description of these various scenarios has focused on the situation where the Fermi energy lies close to the singularity in the density of states. In this paper we wish to do two things. First, we will extend these calculations to all electron densities, in the vicinity of the singularity, and well away from it. Our results will be numerical, and will account self-consistently for changes in the chemical potential as the electron density and coupling strength of the pairing interaction varies. These calculations will be performed for a two-dimensional tight-binding model on a square lattice, where a logarithmic singularity in the electronic density of states always exists.

Secondly, we will extend these calculations to three dimensions. Of course, van Hove anomalies also exist in three dimensions. Jelitto [17] showed long ago that for the body-centred-cubic (bcc) and face-centred-cubic (fcc) lattice structures these anomalies result in singularities in the density of states as well. As this important result appears to be underappreciated, we review some of his results in the Appendix. Finally, we note that the density of states for the bcc lattice, with a non-negligible next-nearest-neighbor

(NNN) hopping amplitude, renders a density of states with a significant and "robust" peak, very similar to one recently calculated [18,19] with density functional theory for the newly discovered superconductor, H_3S [20]. We find a significant enhancement of T_c for electron densities obtained for the chemical potential close to the energy of this peak. In summary, while the bulk of this paper is devoted to a comprehensive survey for T_c (and in some cases the isotope coefficient and the superconducting order parameter), as a function of electron density and coupling strength, in both two and three dimensions, for a variety of "cubic" lattice structures, we find that the bcc structure itself results in a substantial enhancement of T_c.

It is probably best to specify the following simplifying assumptions that we utilize. (i) We assume a momentum independent pairing interaction, and hence this study is confined to a superconducting order parameter with s-wave symmetry. (ii) We will adopt a nonretarded framework for the interaction, i.e., we will use the BCS formalism, rather than the Eliashberg formalism. Many authors (see, e.g., Ho *et al.* [6]) have pointed out that retardation effects will smear the effective electronic density of states, so that a BCS-like treatment will tend to overestimate the effects of a singularity in the density of states. This is understood here, and it is desirable to have a follow-up study similar to this one based on the Eliashberg formalism [21]. (iii) We will focus on a metal in which a single band crosses the Fermi level; furthermore, we will adopt a tight-binding model to describe the dispersion of this band, and correlation effects in the normal state are assumed to be absent. (iv) While we will adopt analytical approximations from time to time these will be for illustrative purposes only—all our main results will be numerically exact, with no weak coupling approximations, for example. The one exception is that at the band edges we do not concern ourselves with possible strong coupling effects. These effects will give rise to Bose condensation physics dominating over BCS pairing (i.e., condensation arises not from pairing *per se*, but from phase coherence); however, since the theoretical description of this crossover is not universally agreed upon [22,23], for present purposes we simply use the BCS formalism in this very small regime as well.

The outline is as follows. In the next section we provide a concise formulation of the equations we solve, both at the critical temperature T_c, and at temperatures below T_c. In the following section we focus on the two-dimensional square lattice, first with nearest-neighbor hopping only, and then with next-nearest-neighbor hopping. We examine $T_c = T_c(n,V,\omega_D)$, where n is the electron density, V is the coupling strength, and ω_D is used as a cutoff, representing the Debye frequency of the phonons. We also examine the isotope coefficient (to be defined below) and the superconducting order parameter, Δ. For the most part $\Delta(n,V,\omega_D)$ tracks $T_c(n,V,\omega_D)$, and the temperature dependence of Δ is essentially indistinguishable from that achieved with a constant density of states. Results for a constant density of states have previously been presented [24] within the Eliashberg [25,26] formalism. These results, recalculated with the much simpler BCS formalism, will provide a baseline for comparisons.

The fourth section will focus on the three-dimensional cubic lattices: simple cubic (sc), body-centered cubic (bcc), and face-centered cubic (fcc). The first two have particle-hole symmetry, while the third does not, and the singularity in the electron density of states for the fcc lattice lies at the upper end of the spectrum. We also consider the impact of next-nearest-neighbor hopping in all three cases. Somewhat surprisingly, in the bcc and fcc cases, while the singularity is removed, a robust peak remains, and considerable enhancement of T_c occurs. Equally surprisingly, in the sc case, turning on the next-nearest-neighbor hopping moves the density of states towards one with a singularity.

Finally, we point out that for a particular range of NNN hopping amplitude, the density of states resembles that calculated [27,28] with density functional theory, and leads to a significant enhancement of T_c.

II. PAIRING FORMALISM

The BCS equations are written as [29,30]

$$\Delta_k = -\frac{1}{N}\sum_{k'} V_{kk'}\frac{\Delta_{k'}}{2E_{k'}}[1-2f(E_{k'})] \tag{2}$$

and

$$n = \frac{1}{N}\sum_{k'}\left[1-\frac{\epsilon_{k'}-\mu}{E_{k'}}[1-2f(E_{k'})]\right], \tag{3}$$

with

$$E_k \equiv \sqrt{(\epsilon_{k'}-\mu)^2+\Delta_{k'}^2}. \tag{4}$$

Here, Δ_k is the superconducting order parameter; this parameter goes to zero at the critical temperature T_c. N is the number of unit cells in the lattice and the summation over k points is to cover the entire first Brillouin zone (FBZ). In principle this summation also covers all bands in the FBZ, but as specified in our assumptions we focus on one band only, in which the Fermi energy lies. The pairing interaction, to be specified further below, is given by $V_{kk'}$. Note that the dependence on the center-of-mass momentum q is absent, so that this is the interaction for the so-called "reduced BCS" Hamiltonian. We have also adopted the convention that an attractive interaction will be negative, so that Eq. (2) has a minus sign. The chemical potential is denoted by μ; it will generally be altered by the presence of the superconducting state, although in practice, in weak and intermediate coupling situations it will change only by a very small amount. By using Eq. (3) we take these changes into account in order to preserve the electron density, n, as the various parameters, such as temperature, or even the "fixed" parameters like ω_D, are varied. Finally all the temperature dependence is included through the Fermi-Dirac distribution function, $f(x) \equiv 1/[\exp(\beta x)+1]$, where $\beta \equiv 1/[k_B T]$ is the inverse temperature, with k_B the Boltzmann constant.

In addition we need to specify an energy dispersion, ϵ_k. We adopt the tight-binding model, so for example, with nearest-neighbor (NN) hopping only, we obtain

$$\epsilon_k = -2t[\cos(k_x a)+\cos(k_y a)] \quad \text{[2D]}, \tag{5}$$

$$\epsilon_k = -2t_s[\cos(k_x a)+\cos(k_y a)+\cos(k_z a)] \quad \text{[sc]}, \tag{6}$$

$$\epsilon_k = -8t_b\left[\cos\left(\frac{k_x a}{2}\right)\cos\left(\frac{k_y a}{2}\right)\cos\left(\frac{k_z a}{2}\right)\right] \quad \text{[bcc]}, \tag{7}$$

$$\epsilon_k = -4t_f\left[\cos\left(\frac{k_x a}{2}\right)\cos\left(\frac{k_y a}{2}\right) + \cos\left(\frac{k_x a}{2}\right)\cos\left(\frac{k_z a}{2}\right) + \cos\left(\frac{k_y a}{2}\right)\cos\left(\frac{k_z a}{2}\right)\right] \quad \text{[fcc]} \tag{8}$$

for the four structures considered, where a is the nearest-neighbor distance in the 2D and (sc) cases, and is the length of the cube in the bcc and fcc cases, containing eight atoms at each vertex along with one in the center (bcc) and six on the face centers (fcc). Also, t, t_s, t_b, and t_f are the nearest-neighbor hopping parameters for the 2D square, 3D simple cubic, 3D bcc, and 3D fcc lattices, respectively. Note that these have bandwidths W of $8t$, $12t_s$, $16t_b$, and $16t_f$, respectively. In the main text and figures that follow, we will generally use "t" to designate the NN hopping, and "t_2" to designate the next-nearest-neighbor (NNN) hopping parameter (see the Appendix). Thus, unless necessary to distinguish the various cases, we will drop the additional subscript, s, b, and f, and retain them only as needed. These dispersions are further discussed in the Appendix.

At this point the main simplifying assumption in the ensuing calculations is that the pairing interaction is essentially local, so that the pairing interaction is independent of momentum. We wish to retain the notion that pairing is via boson exchange, and with the phonon mechanism in mind following BCS [1], we want to include a feature that requires the two electrons to have single particle energies that are no further than $\hbar\omega_D$ apart from one another. This is difficult to implement in practice, so instead we adopt the standard model that restricts each of the single particle energies to be within $\hbar\omega_D$ of the chemical potential, μ. That is,

$$V_{kk'} = -V\theta[\hbar\omega_D - |\epsilon_k - \mu|]\theta[\hbar\omega_D - |\epsilon_{k'} - \mu|], \tag{9}$$

where $\theta[x] \equiv 0$ for $x < 0$ and $\theta[x] \equiv 1$ for $x > 0$ is the Heaviside step function, and $V > 0$ implies that this is an attractive interaction potential. With this model in place, the order parameter becomes nonzero only for $|\epsilon_k - \mu| < \hbar\omega_D$, and its value is independent of momentum [31].

Because of the simplicity of this model potential, one can rewrite the momentum sums in Eqs. (2,3) in terms of the electronic density of states, $g(\epsilon)$ (see the Appendix). Then these equations become

$$\frac{1}{V} = \int_{\mu_-}^{\mu_+} d\epsilon\, g(\epsilon)\frac{\tanh[\beta E(\epsilon)/2]}{2E(\epsilon)} \tag{10}$$

and

$$n = \int_{\epsilon_{\min}}^{\epsilon_{\max}} d\epsilon\, g(\epsilon)\left[1 - \frac{(\epsilon-\mu)}{E(\epsilon)}\tanh[\beta E(\epsilon)/2]\right], \tag{11}$$

with $E(\epsilon) = \sqrt{(\epsilon-\mu)^2 + \Delta^2}$. Here, the integration limits in Eq. (10) are normally $\mu_- = \mu - \hbar\omega_D$ and $\mu_+ = \mu + \hbar\omega_D$, while those in Eq. (11) are $\epsilon_{\min}$, the band energy at the bottom of the band, and $\epsilon_{\max}$, the band energy at the top of the band. An exception occurs when the chemical potential is close to one of the band edges. In this case, the integration is cut off by the band edge, so more accurately, $\mu_- \equiv \max[\mu - \hbar\omega_D, \epsilon_{\min}]$, and $\mu_+ \equiv \min[\mu + \hbar\omega_D, \epsilon_{\max}]$.

Equations (10) and (11) represent two nonlinear equations for the unknowns Δ and μ, given the parameters V and n. At zero temperature the hyperbolic tangent function is replaced by unity; at T_c the order parameter goes to zero so the problem is slightly different. One then has to find the temperature and the chemical potential at which both these equations are satisfied. These equations are

$$\frac{1}{V} = \int_{\mu_-}^{\mu_+} d\epsilon\, g(\epsilon)\frac{\tanh[\beta_c(\epsilon-\mu)/2]}{2(\epsilon-\mu)} \quad [T = T_c] \tag{12}$$

and

$$n = 2\int_{\epsilon_{\min}}^{\epsilon_{\max}} d\epsilon\, g(\epsilon) f(\epsilon - \mu) \quad [T = T_c], \tag{13}$$

where $\beta_c \equiv 1/[k_B T_c]$. Numerical results in subsequent sections are the result of an iterative solution to these equations.

III. TWO DIMENSIONS

As detailed in the Appendix, the electron density of states for a two-dimensional tight-binding model with nearest-neighbor hopping only is

$$g_{2D}(\epsilon) = \frac{1}{2\pi^2 t a^2} K\left[1 - \left(\frac{\epsilon}{4t}\right)^2\right], \tag{14}$$

where $K(m) \equiv \int_0^{\pi/2} d\theta (1 - m\sin^2\theta)^{-1/2}$ is the complete elliptic integral of the first kind [32]. This density of states is well approximated by the expression

$$g_{2D}(\epsilon) \approx \frac{1}{2\pi^2 t a^2}\log\left(\frac{16t}{|\epsilon|}\right). \tag{15}$$

Equation (15) is the asymptotic form of Eq. (14) as $\epsilon \to 0$, and is often used in lieu of Eq. (14). Both are shown in Fig. 13 in the Appendix, along with a numerical evaluation of the density of states when the next-nearest-neighbor hopping is included as well. As discussed in the Appendix, a simple numerical routine can efficiently and accurately evaluate complete elliptic integrals, so we proceed with the full form, Eq. (14).

A. Numerical results

We show in Fig. 1(a) T_c/ω_D (we set $\hbar = k_B = 1$) vs electron density n, for a relatively weak coupling situation, $V/t = 2$, for three different values of $\omega_D/t = 1.0$, 0.1, and 0.01. The latter two values are more realistic as in general, $\omega_D \ll t$, i.e., phonon energy scales are much smaller than electronic energy scales. The curves provide results for the complete self-consistent solution without approximation, i.e., using the density of states from Eq. (14). There is a clear enhancement of T_c, especially near the van Hove singularity. and the enhancement is most pronounced for smaller values of ω_D. Also shown is the result for a constant density of states; for electron densities near half-filling this shows that T_c can be enhanced by more than an order of magnitude. In Fig. 1(b) we show the same quantity as a function of ω_D/t, now for a variety of values of V/t, all for half-filling (shown with curves). T_c will tend to increase as a function of ω_D, but we have plotted

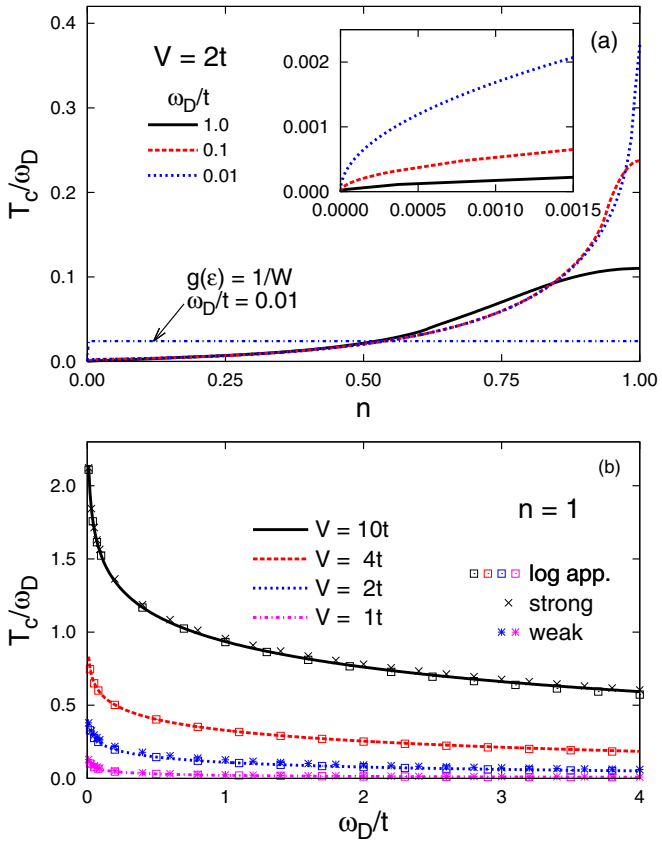

FIG. 1. (a) Plot of T_c/ω_D vs n for $0 < n < 1$ (the results for $2 > n > 1$ are symmetric) for $V/t = 2$, and $\omega_D/t = 1.0, 0.1, 0.01$. Also shown is the result for a constant density of states, $g(\epsilon) = 1/W$, where $W = 8t$ is the electron bandwidth. This result is not sensitive to ω_D except at the band edges. In the inset we show an expanded view of the region near zero density (also the case near $n = 2$), showing how $T_c \propto \sqrt{n}$ due to the lower band edge taking the place of $\mu - \omega_D$ for the lower cutoff. There is a clear enhancement near the van Hove singularity, especially for small ω_D/t. (b) T_c/ω_D vs ω_D/t for $n = 1$ for several values of the coupling strength V, along with several approximations discussed in the text.

the ratio, T_c/ω_D vs ω_D/t, which shows an enhancement of T_c/ω_D as $\omega_D \to 0$.

B. Analytical results

Analytical results are possible through a series of simplifications, as follows. First, we focus on half-filling, $n = 1$. This means that the chemical potential remains fixed at $\mu = 0$, independent of temperature. Second, we adopt the approximation given in Eq. (15), which, based on the comparisons of the density of states given in the Appendix, we anticipate will be very accurate. Indeed, this is the case, as indicated by the results depicted with square symbols in Fig. 1(b). In particular, these results are always very accurate as $\omega_D \to 0$, as this is where the density of states at the singularity is most important; this is also where the approximation Eq. (15) is most accurate.

A so-called "strong-coupling" approximation to the BCS equation is obtained as follows. We assume $\omega_D/T_c \ll 1$, which means that the hyperbolic tangent function can be linearized. The remaining integral is then elementary, so that

$$\frac{T_c}{\omega_D} \approx \frac{V}{4\pi^2 t}\left[\log\left(\frac{16t}{\omega_D}\right) + 1\right] \quad \text{[strong coupling]}. \tag{16}$$

These results are indicated with x's, and only for $V = 10t$ in Fig. 1(b), where it is seen to be very accurate. Here we caution the reader that it is an accurate approximation to the fully self-consistent solution as indicated, but in fact BCS theory itself is not expected to be very accurate in this regime at finite temperature. So here it merely serves as a check that our solutions to the equations are accurate.

The opposite case, that of weak coupling, is the one most normally used; furthermore, we expect BCS theory to be reasonably accurate, at least in three dimensions. In two dimensions, these results are also generally not so accurate, because Kosterlitz-Thouless physics [37] is expected to come into play. Our approximation follows the standard one [30], but accommodates the density of states with the logarithm singularity [Eq. (15)]; we obtain

$$\frac{T_c}{\omega_D} \approx 1.134 \exp\left\{A - \sqrt{A^2 + \frac{4\pi^2 t}{V} - B - \log[2(1.134)]}\right\} \tag{17}$$

(weak coupling), where

$$A \equiv A(\omega_D/t) \equiv 1 + \log\left(\frac{8t}{1.134\omega_D}\right) \tag{18}$$

and

$$B \equiv \int_0^\infty dx\, \mathrm{sech}^2 x \log^2 x \approx 1.989\ldots. \tag{19}$$

These results are indicated with asterisks for $V = 2t$ and $V = 1t$ in Fig. 1(b), where they are indeed very accurate. Although not shown, they become less accurate as V increases. Notice, however, that even for $T_c/\omega_D \approx 0.4$ ($V = 2t$ and $\omega_D \to 0$) the weak coupling approximation works very well. Equation (17) is useful to illustrate how the logarithmic singularity in the density of states changes the usual exponential suppression for superconducting T_c to one that can be significantly enhanced, as now the *square root* of the inverse coupling strength appears in the exponential, a fact first pointed out, to our knowledge, in Ref. [10]. This is most readily seen by allowing $V/t \to 0$ in Eq. (17), to get

$$\frac{T_c}{\omega_D} \approx 1.134 \exp\left\{-\sqrt{\frac{4\pi^2 t}{V}}\right\}. \tag{20}$$

C. Beyond nearest-neighbor hopping

Going beyond nearest-neighbor hopping in two dimensions destroys the particle hole symmetry, but the singularity in the density of states remains, albeit at some different value for the chemical potential (i.e., filling). The Appendix displays the density of states for various values of the next-nearest-neighbor (NNN) hopping parameter. Figure 2 shows T_c/ω_D vs filling and again illustrates that a significant enhancement occurs when the chemical potential is close to the van Hove singularity.

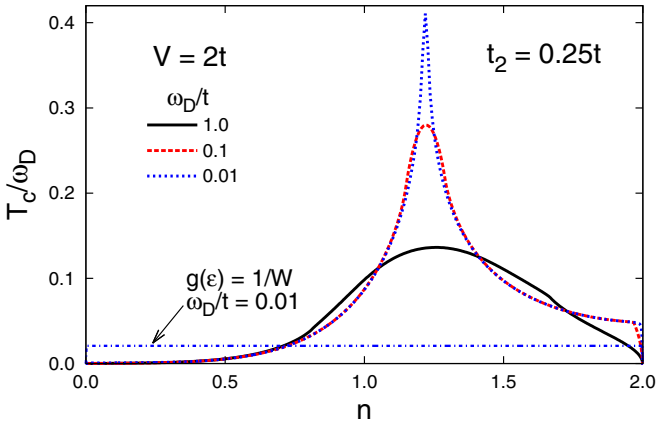

FIG. 2. Plot of T_c/ω_D vs n for $V/t = 2$, and $\omega_D/t = 1.0,0.1,0.01$, for the 2D case where next-nearest-neighbor (NNN) hopping is also present. The van Hove singularity is now located at $\epsilon = 4t_2$ which corresponds to a filling $n \approx 1.2$. Also shown is the result for a constant density of states, $g(\epsilon) = 1/W$, where $W = 8t$ is the electron bandwidth. The same enhancement occurs as when NNN hopping is not included, when the chemical potential approaches the energy of the van Hove singularity. As was the case in Fig. 1 the enhancement of T_c/ω_D is amplified as ω_D decreases.

D. Isotope effect

The partial isotope coefficient is defined by [25]

$$\beta_i \equiv -\frac{d\ln T_c}{d\ln M_i}, \tag{21}$$

where M_i is the mass of the ith element; the total isotope coefficient (β) is the sum of these, and for the purpose of this work we will assume an elemental superconductor; furthermore, for the harmonic approximation $\omega_D \propto 1/\sqrt{M}$, Eq. (1) implies the expected standard result, $\beta = 1/2$. This positive value indicates that increasing the Debye frequency is expected to raise T_c.

The presence of a nonconstant density of states will quantitatively change this result; in particular, if the chemical potential is at a van Hove singularity, then decreasing the mass (i.e., increasing the Debye frequency) will increase T_c less than what one would expect normally. This is because more states are included in the energy-lowering due to condensation, as before, but the energy regime where this occurs (about ω_D on either side of the chemical potential) has a lower electronic density of states, so the incremental benefit is decreased from what it is if the density of states is constant.

Figure 3 shows the isotope coefficient vs ω_D/t for (a) nearest-neighbor (NN) hopping only, at half-filling, (b) NNN with the chemical potential at the van Hove singularity ($n = 1.219$), and (c) NNN with a filling of $n = 1.5$. The results in Figs. 3(a) and 3(b) are qualitatively similar; the coefficient rapidly decreases as ω_D increases, as would be expected, since the relevant energy regime moves further away from the singular part of the density of states with increasing ω_D. In both cases a precipitous drop occurs when ω_D exceeds a value that corresponds to the distance from the chemical potential to the band edge. While these values are unrealistically large, it is worth understanding what is occurring. In the case of

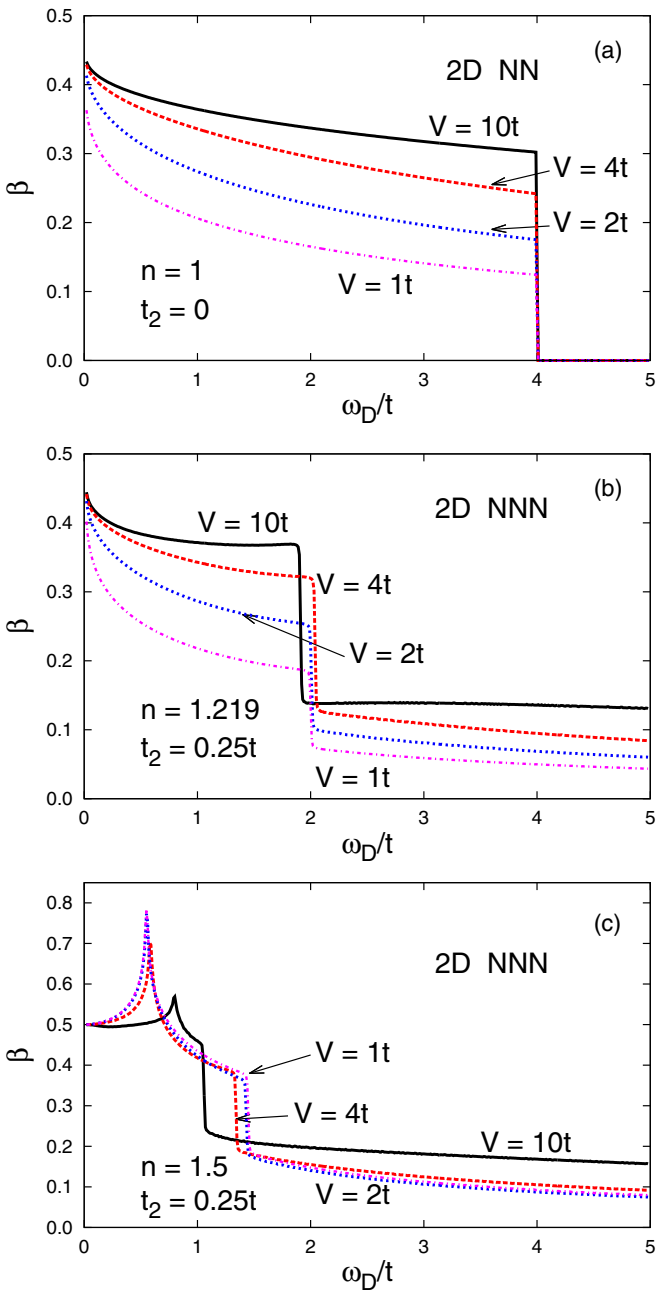

FIG. 3. Isotope coefficient β vs ω_D/t for (a) NN hopping only and $n = 1$, (b) NNN hopping with $t_2 = 0.25t$ and $n = 1.219$, and (c) NNN hopping, again with $t_2 = 0.25t$, but with $n = 1.5$. In (a) and (b) the filling is such that the chemical potential is at the van Hove singularity. In both these cases the behavior is qualitatively similar and the isotope coefficient decreases as a function of ω_D/t (note that the physically relevant regime is $\omega_D/t \ll 1$). Moreover, the most significant decrease occurs in both instances for weaker coupling, which is where BCS theory is to be most trusted. In (c) the chemical potential is away from the van Hove singularity. This results in a peak in the isotope coefficient, at a value of ω_D which tracks the energy difference between the chemical potential and the van Hove singularity. This is as expected, as the highest impact on T_c will occur when the value of ω_D can include the states at the van Hove singularity. At large (and unrealistic) values of ω_D the isotope coefficient decreases significantly as two (a) or one [(b) and (c)] band edges replace ω_D as the cutoff.

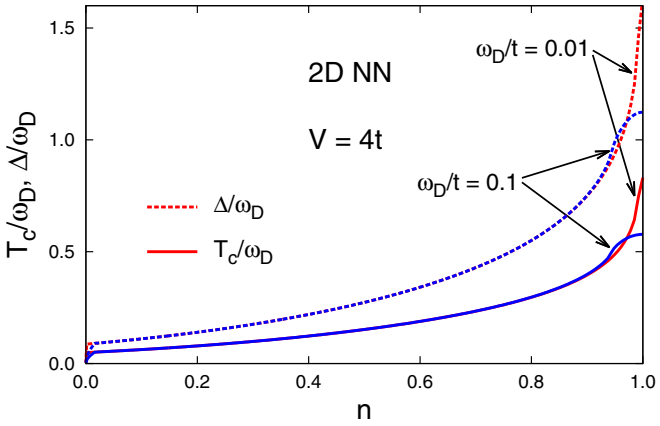

FIG. 4. T_c and the zero temperature order parameter, Δ, vs electron density n, for the 2D case with NN hopping only, with $V = 2t$ and $\omega_D = 0.1t$. The behavior of Δ follows that of T_c, with a slight enhancement of the ratio as the singularity is approached.

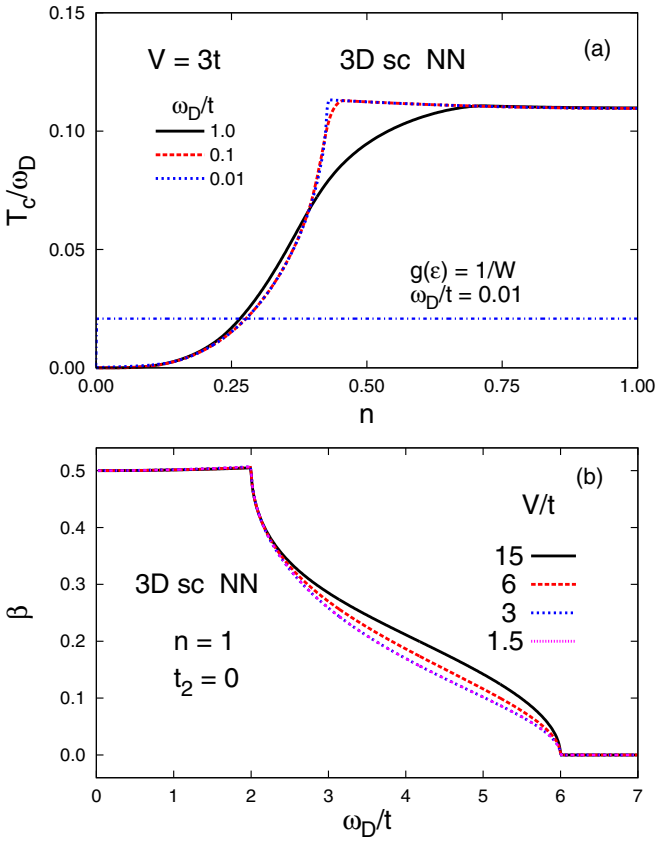

FIG. 5. (a) T_c vs filling, n, and (b) the isotope coefficient β vs ω_D/t for a variety of values of ω_D in (a) and for a number of coupling strengths in (b). These results are for the simple cubic three-dimensional case, with NN hopping only, and for $n = 1$. Results are as expected and as explained in the text.

NN hopping this value is $4t$, and then the isotope coefficient becomes zero, since further increasing ω_D plays no role in determining T_c, as the role of the cutoff is now taken by the band edge, and not ω_D. For NNN hopping only one band edge takes on the role of the cutoff; the second bandwidth will enter for larger values of ω_D/t than those shown.

In Fig. 3(c) the chemical potential is well away from the van Hove singularity; then the isotope coefficient β peaks in value when the value of ω_D is "tuned" to equal the difference in energy between the chemical potential and the energy of the van Hove singularity. Coupling to these states has the most significant effect on T_c, which results in a peak and in the achievement of anomalously high values of β.

E. Zero temperature energy gap

One can ask if the just-described effects of a van Hove singularity similarly apply to the finite temperature energy gap. We have thus solved the finite temperature gap equations, Eqs. (10) and (11), in several representative cases. For the most part we find that little differs for the pairing gap, Δ, as a function of vicinity of the Fermi energy to the van Hove singularity. For example, the temperature dependence, $\Delta(T)$, as a function of temperature T is barely discernible from the usual temperature dependence obtained with a constant density of states. By way of example, we show in Fig. 4 the pairing gap at zero temperature, Δ, and the superconducting critical temperature, T_c, as a function of electron density, n, for the 2D case with NN hopping only. Both peak near $n = 1$, i.e., the location of the van Hove singularity in the density of states; in this sense, Δ tracks T_c. The ratio, for example, $2\Delta/(k_B T_c)$, grows from 3.53 at low densities to about 3.7 at half-filling, a rather insignificant change. We turn to three dimensions now, and focus on T_c.

IV. THREE DIMENSIONS

We now turn to similar calculations in 3D. As summarized in Eqs. (6)–(8), we focus only on the cubic lattice structures, sc, fcc, and bcc. The densities of states for these were first calculated by Jelitto [17] and are provided in the Appendix for cases involving NNN hopping as well. As we mentioned earlier, while these calculations were performed almost half a century ago, most researchers are not aware [33] that singularities indeed exist in the tight-binding model for the bcc and fcc cases (for NN hopping only) and even in the sc case when NNN hopping is included. This is true only for "special" values of the hopping parameters, but as detailed in the Appendix, remnants of these singularities remain even when other values of the hopping parameters are used. Based on what we found in two dimensions, along with some exploratory calculations, here we will focus on T_c and the isotope coefficient, β; results for Δ follow those of T_c, as we found in two dimensions.

A. Simple cubic NN

The simple cubic density of states consists of van Hove singularities only in the derivative of the density of states with respect to energy (see the red curve in Fig. 14 in the Appendix). The behavior of T_c is therefore not so unusual. Figure 5(a) shows T_c/ω_D vs n for a fairly weak coupling case ($V = 3t$) from zero density to half-filling ($n = 1$). Note that this lattice is bipartite and has particle-hole symmetry. Hence results for $n > 1$ are a mirror reflection of those for $n < 1$, and we display

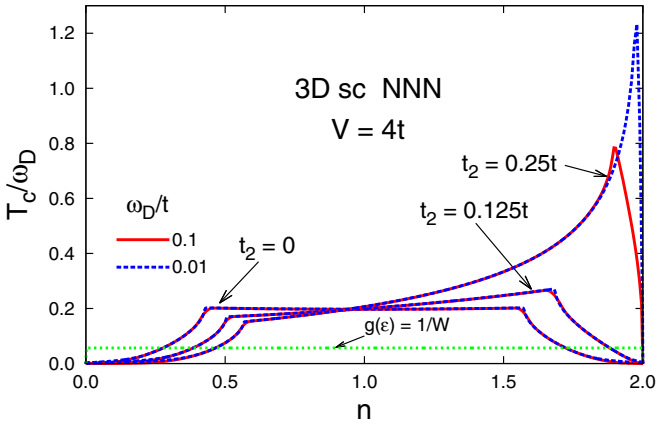

FIG. 6. Plot of T_c/ω_D vs n for $V/t = 4$, and $\omega_D/t = 0.1,0.01$, for three different values of $t_2/t = 0,0.125,0.250$. Note that the results are relatively insensitive to ω_D except for $t_2 = 0.25t$, where a singularity exists in the density of states near the top of the band (see Fig. 14 in the Appendix), and T_c/ω_D continues to increase near $n = 2$ as ω_D decreases. Also shown is the result for a constant density of states, $g(\epsilon) = 1/W$, where $W = 12t$ is the electron bandwidth for the sc lattice with $|t_2|/t \leqslant 1/4$. This latter result is not sensitive to ω_D except at the band edges, and is shown only for $\omega_D/t = 0.01$.

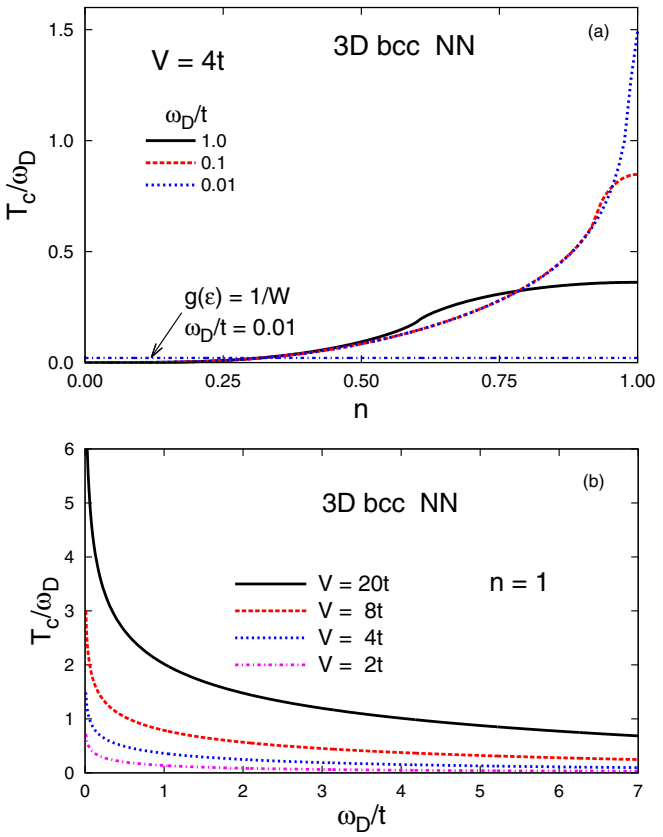

FIG. 7. (a) Plot of T_c/ω_D vs n for $0 < n < 1$ (the results for $2 > n > 1$ are symmetric) for $V/t = 4$, and $\omega_D/t = 1.0,0.1,0.01$. Also shown is the result for a constant density of states, $g(\epsilon) = 1/W$, where $W = 16t$ is the electron bandwidth. This latter result is not sensitive to ω_D except at the band edges. There is a significant enhancement near the van Hove singularity, which continues to grow without bound for decreasing ω_D/t. (b) T_c/ω_D vs ω_D/t for $n = 1$ for various values of V. This view highlights the sharp increase in T_c/ω_D as $\omega_D \to 0$.

only the latter. We show results for three values of ω_D; in fact as long as $\omega_D \ll t$ the electron density of states at the chemical potential plays the most important role, as is evident from how T_c tracks $g(\epsilon_F)$, albeit as a function of occupation rather than as a function of energy. Only for $\omega_D = t$ does the T_c curve begin to become "rounded" compared to the density of states. Also shown is the result obtained for a constant density of states, $1/W$, where $W = 12t$ for the three-dimensional simple cubic tight-binding model. In Fig. 5(b) we show the isotope coefficient as a function of ω_D/t for four different values of the coupling strength, V/t. The results for $V = 3t$ and $V = 1.5t$ cannot be distinguished from one another, indicating that $V = 3t$ is already in the weak coupling limit. The isotope coefficient becomes reduced from the "canonical" value of 0.5 only when ω_D increases beyond the energy of the first van Hove singularity near the origin, at $\pm 2t$. The β decreases steadily to zero, achieved for $\omega_D \geqslant W/2 = 6t$. The dependency on coupling strength is very minor. Away from half-filling there are no surprises, and both T_c and β track the density of states at the chemical potential. As was the case in two dimensions, the isotope coefficient displays a peak when the size of ω_D allows a coupling to states with significantly higher density of states, i.e., when $|\mu| > 2t$, where μ is the chemical potential.

B. Simple cubic NNN

Remarkably, including sufficient NNN hopping in the sc lattice results in a singularity in the density of states at the top of the band (see the blue curve in Fig. 14 in the Appendix), similar to what occurs for the fcc lattice with NN hopping only (see below). In Fig. 6 we show T_c/ω_D vs electron density for three different values of the NNN hopping, $t_2/t = 0,0.125,0.250$ and two different values of ω_D. The value of ω_D is not so important except in the case $t_2/t = 0.25$, where a singularity occurs in the density of states; this results in a singularity in T_c/ω_D near $n = 2$ as ω_D decreases. Also shown is the result for a constant density of states with value $g(\epsilon) = 1/W$, where $W = 12t$ is the electron bandwidth for the sc lattice with $|t_2|/t \leqslant 1/4$. Clearly the potential enhancement of T_c/ω_D is very large at high fillings. A particle-hole symmetry exists with these results for negative values of t_2/t (not shown). The important point is that for values of t_2/t close to 0.25 a peak will remain in the density of states, giving rise to a large enhancement in T_c/ω_D.

C. Body-centered cubic NN

As noted in the Appendix the tight-binding model with a bcc lattice with NN hopping only displays a singularity at $\epsilon = 0$. This singularity is a logarithm squared and hence stronger than the two-dimensional singularity which diverges logarithmically. Figure 7(a) shows T_c/ω_D vs n for a fairly weak coupling case ($V = 4t$) for zero density to half-filling ($n = 1$). Like the sc 3D case, the bcc lattice is bipartite, and with NN hopping only, this lattice has particle-hole symmetry. Hence, as in that case, results for $n > 1$ are a mirror reflection of those for $n < 1$, and we display only the latter. We show results for three values of ω_D; again, as long as $\omega_D \ll t$, the

electron density of states at the chemical potential plays the most important role. In particular, for the smallest value of ω_D shown, T_c again tracks $g(\epsilon_F)$ as a function of occupation (rather than as a function of energy). The enhancement above the result for a constant density of states with the same bandwidth (horizontal line just above zero) is enormous. Here, $W = 16t$ for the bcc NN tight-binding model. In Fig. 7(b) we show the same quantity, T_c/ω_D vs ω_D, for a variety of coupling strengths at half-filling. As expected, this BCS calculation shows T_c increasing with V; we remind the reader again that this calculation is expected to be valid only for some weak coupling range. The important point is that T_c/ω_D eventually diverges as ω_D decreases, because the density of states at $\mu = 0$ is diverging, and the density of states right at the Fermi level becomes the only key quantity as the Debye frequency decreases.

Away from half-filling results are again as expected; the chemical potential is at an energy where the density of states is relatively low. As ω_D increases to a point where the singularity in the density of states becomes relevant, then T_c/ω_D will peak. Unlike Fig. 7(b), where T_c/ω_D monotonically decreases as ω_D increases, T_c/ω_D is nonmonotonic, i.e., the result is sensitive to the singularity *not at* the Fermi level.

The isotope coefficient is similar to what we have seen before; in Fig. 8(a) we show β as a function of ω_D/t for $n = 1$ and for a variety of coupling strengths. Clearly the isotope coefficient is greatly reduced even for fairly low values of ω_D/t. In Fig. 8(b) we show the same result for $n = 0.5$; now the isotope coefficient peaks to very high values, as values of ω_D are reached that bring the singularity in the electron density of states in "resonance" with the chemical potential through ω_D. That is, a prominent peak in β occurs, particularly in weak coupling, when $\mu + \omega_D = \epsilon_{\text{sing}}$, where $\epsilon_{\text{sing}} = 0$ is the energy at which the singularity occurs. We thus have the intriguing possibility of an anomalously high isotope coefficient associated with a nonoptimal critical temperature.

The bcc tight-binding model shows significant enhancement for T_c, for a wide range of electron density [Fig. 7(a)]. However, as was the case in 2D, it is important to examine the impact of a NNN hopping parameter. We do this in the next subsection.

D. Body-centered-cubic NNN

The introduction of NNN hopping for the bcc lattice structure changes the nature of the density of states in a profound way. As illustrated in the Appendix, the singular behavior is entirely removed. Nonetheless, a highly peaked structure remains, which we expect will continue to cause a considerable enhancement of T_c. This enhancement is more significant than the one found at half-filling since the Fermi surface is no longer nested, and therefore competing instabilities to superconductivity will be suppressed. Since the density of states is not singular, however, we expect that T_c will *not* continue to increase as ω_D is decreased [as was the case in Fig. 7(a) at $n = 1$]. Nonetheless, as noted in the Appendix, the maximum is, in many respects, more "robust" than in the NN case, in that a larger area is contained in the maximum region than in the NN case. This was also the case in 2D, and is the case for the fcc lattice structure (see Fig. 16 below).

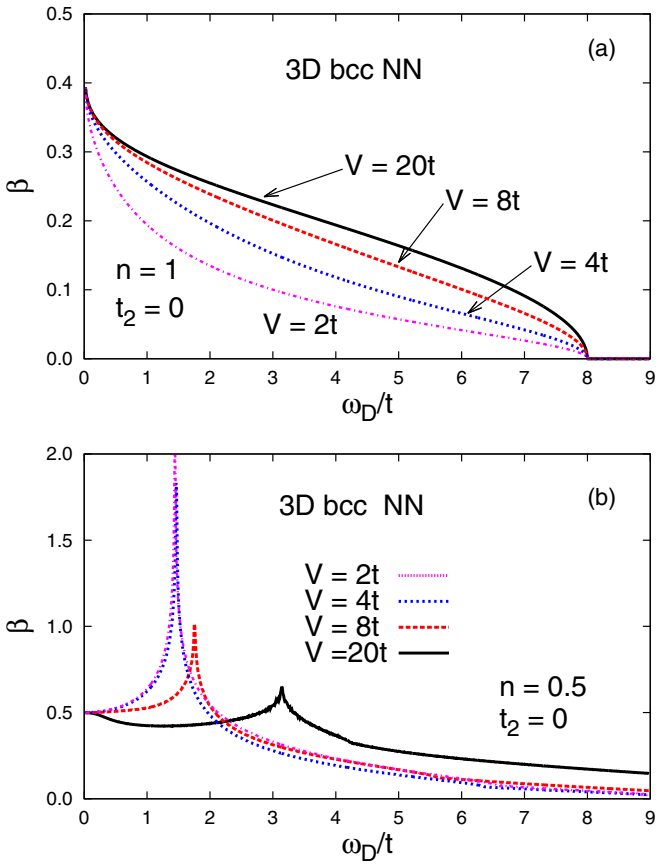

FIG. 8. (a) Isotope coefficient β vs ω_D/t for the 3D bcc NN case ($t_2 = 0$), at half-filling, for a variety of coupling strengths. The isotope coefficient is significantly reduced from 0.5, due to the singularity in the density of states. (b) Isotope coefficient β vs ω_D/t for the 3D bcc NN case ($t_2 = 0$), at quarter filling $n = 0.5$, for the same coupling strengths as in (a). The isotope coefficient now has a significant peak, particularly for weak coupling, when ω_D is such that states in the peak of the density of states are primarily included in determining T_c (see text).

Figure 9 shows T_c/ω_D vs n, for a variety of values of ω_D, for the particular case of $t_2 = 0.3t$. As anticipated, the enhancement with decreasing ω_D now saturates; near the peak values, T_c/ω_D hardly increases as $\omega_D = 0.1t$ (red curve) decreases to $\omega_D = 0.01t$ (blue curve). This is in contrast to the scenario shown in Fig. 7, where, near the peak electron density, T_c/ω_D continues to increase indefinitely as ω_D decreases. Here, however, the Fermi surface is no longer nested, and competing instabilities, not considered here, will be significantly suppressed (see, for example, Fig. 1 in Ref. [36] for a demonstration of the suppression of a charge-density-wave instability due to the removal of nesting). Thus the large enhancement displayed in Fig. 9 will likely remain even when competing instabilities are considered.

E. Face-centered-cubic NN and NNN

Similar to the bcc NN case, the electron density of states for an fcc lattice with NN hopping only also displays a singularity, right at the band edge, as shown by the red curve, i.e., the rightmost curve, in Fig. 16 in the Appendix. In this case the

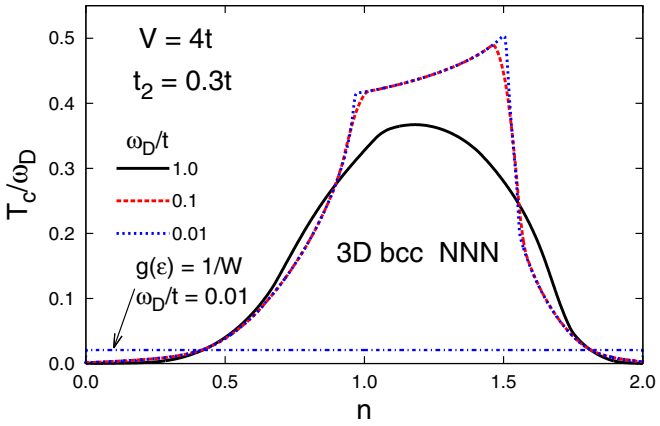

FIG. 9. Plot of T_c/ω_D vs electron density n for $V/t = 4$, for the bcc lattice structure, now with NNN hopping, $t_2 = 0.3t$, and $\omega_D/t = 1.0,0.1,0.01$. Also shown is the result for a constant density of states, $g(\epsilon) = 1/W$, where $W = 16t$ is the electron bandwidth. As before, this latter result is not sensitive to ω_D except at the band edges. There is a clear enhancement of T_c over a wide range of densities near the maximum in the density of states (see Fig. 15). Note, however, that because the density of states is no longer singular, T_c/ω_D now saturates as ω_D decreases (red to blue curve).

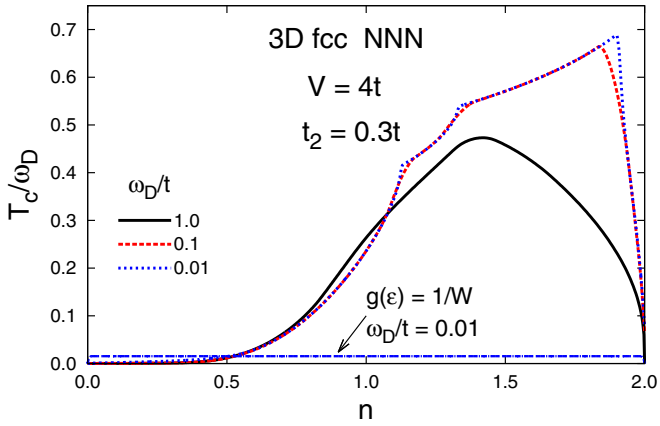

FIG. 11. Plot of T_c/ω_D vs electron density n for $V/t = 4$, for the fcc lattice, now with NNN hopping, $t_2 = 0.3t$, and $\omega_D/t = 1.0,0.1,0.01$. Also shown is the result for a constant density of states, $g(\epsilon) = 1/W$, where $W = 17.2t$ is the electron bandwidth for $t_2 = 0.3t$. Even for the nonconstant density of states results, note the lack of sensitivity of T_c/ω_D to ω_D over essentially all electron densities, for sufficiently small values of ω_D/t. There remains a clear enhancement of T_c/ω_D over a wide range of densities near the maximum in the density of states (see Fig. 16).

FCC lattice is *not* bipartite, so no nesting occurs. In Fig. 10 we show results for relatively weak coupling, $V = 4t$, as a function of electron density, for several values of ω_D. The expected enhancement in T_c/ω_D occurs near the singularity, now at the top of the band, and this increases indefinitely as ω_D decreases. Note that for decreasing ω_D, enhancement of T_c/ω_D continues only for a limited electron density region near the singularity.

This is expected to be a robust result, in that there will not be a large enhancement of competing instabilities due to the lack of nesting. On the other hand, one always expects a small amount of NNN hopping, and as this removes the singularity in the electron density of states, one might well ask whether the ensuing enhancement of T_c/ω_D will also disappear. Figure 16, which also displays the electronic density of states for nonzero values of t_2/t, illustrates that a "robust" peak remains. We focus now on results for $t_2/t = 0.3$. Figure 11 shows T_c/ω_D vs electron density for relatively weak coupling, and shows that a strong enhancement of T_c/ω_D continues to occur near the peak structure in the density of states. In fact the values of T_c/ω_D are comparable to (or even greater than) those achieved (for electron densities $1.0 < n < 1.9$) even with $\omega_D = 0.01t$ in the case with $t_2 = 0$ (see Fig. 10), where a singularity exists in the density of states.

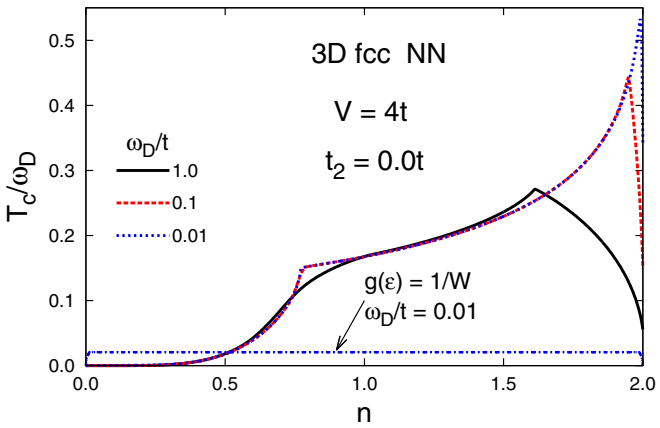

FIG. 10. Plot of T_c/ω_D vs electron density n for $V/t = 4$, for the fcc lattice structure, with NN hopping only, and $\omega_D/t = 1.0,0.1,0.01$. Also shown is the result for a constant density of states, $g(\epsilon) = 1/W$, where $W = 16t$ is the electron bandwidth. As before, this result is not sensitive to ω_D except at the band edges. There is a clear enhancement of T_c over a wide range of densities near the maximum in the density of states (see Fig. 16). Note that, near $n = 2$, this maximum will increase without bound as ω_D decreases.

F. H_3S as a case of bcc with NNN hopping

First-principles calculations show that the Fermi energy occurs near a well-defined peak in the electronic density of states [see Fig. 8 of Ref. [27] and Fig. 2 b or 9 of Ref. [28]]. A very reasonable facsimile of this peak is given by our tight-binding model for the bcc lattice structure with a negative NNN hopping parameter, as shown in the inset of Fig. 12. Not surprisingly, T_c as a function of electron density will display the same peak structure, as illustrated in the main part of Fig. 12 (compare with Fig. 9). While it is not so useful to attempt an actual fit to T_c with such limited data and such a limited theoretical framework (see Ref. [28] for positive steps in removing several of the limitations), for the sake of completeness, we show T_c vs electron density for a number of weak coupling strengths. By way of illustration, for $V = 2t$ [$V/(16t) = 0.125$], with nearest-neighbor hopping $t = 1$ eV, and $\omega_D = 100$ meV (all conservative values), then $T_c \approx 160$ K. We expect actual reductions due to retardation and other effects [28], but these estimates suggest that the

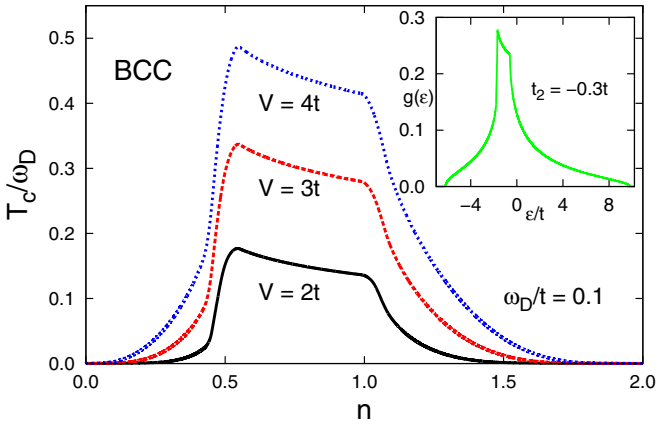

FIG. 12. Plot of T_c/ω_D vs electron density n for various values of coupling strength, $V/t = 2$, 3, and 4. We used the bcc lattice with NNN hopping, $t_2 = -0.3t$, which provides a reasonable facsimile to the peak in the density of states (see inset) calculated with DFT methods. For illustration purposes, if $V = 2t$ $[V/(16t) = 0.125]$, with nearest-neighbor hopping $t = 1$ eV, and $\omega_D = 100$ meV, then $T_c \approx 160$ K (at $n = 1$). In this range of ω_D the results for T_c/ω_D are insensitive to ω_D, and therefore T_c scales with ω_D.

possibility of an enhanced T_c due to a peaked electronic density of states is quite realistic.

V. SUMMARY

In the context of BCS theory, we have examined the role of van Hove singularities in the electronic density of states on the superconducting critical temperature and the isotope coefficient (and briefly the pairing gap) for various band structures given by tight-binding models in two and three dimensions. We have adopted the simplest kind of pairing potential, an attractive interaction with energy scale ω_D, which gives rise to an order parameter with s-wave symmetry. While the model follows the original BCS [1] paper and is therefore suggestive of a phonon-mediated interaction, it in fact has greater generality.

Many such models have been proposed for high temperature superconductors, and many calculations have been performed, as documented in the references. However, here we have gone beyond the existing literature in two respects. First, we have systematically treated the tight-binding models over all electron densities, with careful account of the BCS number equation [our Eq. (3) below T_c or Eq. (11) at T_c], and we have utilized the tight-binding density of states as given, whether for NN hopping only or with NNN hopping included as well. Secondly, we have performed calculations for systems with van Hove singularities in three dimensions. While the simple cubic lattice structure is well known to produce a density of states without singularities (the van Hove singularities manifest themselves in cusps and the derivatives of the density of states), it is less appreciated that both the face-centered cubic and the body-centered cubic exhibit singularities in their densities of states [17]. It is also surprising that the sc lattice structure results in a singular density of states when the NNN hopping t_2 in increased to $t/4$. Well before this value is reached the density of states exhibits a strong peak.

We have illustrated that these singularities can give rise to very large enhancements in T_c. Even in the case of the sc lattice, when NNN hopping is included, significant enhancements of T_c can occur. The bcc lattice is bipartite and therefore nested. As is well known from other nested Fermi surface problems (though certainly less studied for the bcc lattice in particular) other competing instabilities are expected to play an important role, and the BCS calculations provided here become doubtful, as superconducting T_c will often be suppressed. For example, a CDW instability would certainly compete in the case of a bcc lattice, with $\vec{q} = (4\pi/a,0,0)$ along with equivalent wave vectors. Of course, with NNN hopping the CDW instability would likely become incommensurate, and would become suppressed as well. Moreover, this is not an issue with the fcc lattice, as it is not bipartite, the singularity in the density of states in this instance occurs near the top of the band, and other finite q instabilities will not play such a significant role. The possibility still remains that a competing $q = 0$ instability will suppress superconductivity, but consideration of these is beyond the scope of this paper.

Nonetheless, for both the bcc and fcc lattice structures, some NNN hopping is expected, and we have shown here that this immediately leads to the disappearance of the singularity in the density of states. In fact, a "robust" peak remains in the density of states, and as we have shown, a very large enhancement of T_c continues to be present, now in a regime where the BCS calculation is more trustworthy, at least for the bcc lattice structure. This is true for several reasons—for example, as discussed competing instabilities will be suppressed, but in addition, narrow structures in the density of states will be smeared both by impurities, and by retardation effects not accounted for in our BCS calculations. Given the number of superconductors with the fcc and bcc lattice structures, it would be interesting to perform a survey to see if there is any correlation between their critical temperatures and the "remnants" of these van Hove singularities. In fact, the recent discovery of superconducting hydrogen sulfide under high pressure by Drozdov *et al.* [20] has motivated theoretical work [27] that has identified a van Hove singularity in the electronic density of states. The underlying lattice structure is bcc and thus far the origin of this singularity is not clear. This work, particularly the previous subsection, strongly suggests that ultimately the origin of the singularity (and ultimately an important factor in the high superconducting critical temperature) may in fact be bcc structure of the material, along with circumstances that place the Fermi energy in the vicinity of the robust peak that remains even when NNN hopping is included.

We have also computed the isotope coefficient in a variety of cases. It is clear that anomalies in this coefficient will exist due to peaks in the density of states. In some respects the few observations where anomalies are found in known superconductors can be regarded as signatures of peaks in the density of states (although of course other explanations also exist). We have also briefly examined the pairing gap, but there is no significant deviation from what standard BCS theory predicts, i.e., the gap tracks the critical temperature.

ACKNOWLEDGMENTS

This work was supported in part by the Natural Sciences and Engineering Research Council of Canada (NSERC). T.X.R.S. is a recipient of an "Emerging Leaders in the Americas Program" (ELAP) scholarship from the Canadian government, and we are grateful for this support.

APPENDIX: DENSITY OF STATES WITHIN TIGHT BINDING

The general equation for the density of states (DOS) is

$$g(\epsilon) = \frac{1}{N}\sum_{k\in \mathrm{FBZ}} \delta(\epsilon - \epsilon_k), \tag{A1}$$

where ϵ_k is the dispersion relation, the summation is over all points in the first Brillouin zone (FBZ), and N is the number of k points in the FBZ. Dispersion relations are determined by overlap integrals and geometry; for a Bravais lattice the dispersion relation can be written as

$$\epsilon_k = -\sum_{\delta} t_\delta \cos\vec{k}\cdot\vec{\delta}, \tag{A2}$$

where the sum is over all neighbors of a particular lattice site, with decreasing amplitude t_δ, to reflect the decreasing overlap between atoms that are further apart from one another. This decrease with distance is usually exponential, so very often only nearest-neighbor overlaps are considered to be nonzero. It turns out that this simplified model often possesses special symmetries, not necessarily inherent in the more general model, and therefore, if for no other reason, further than nearest-neighbor overlaps are often considered as well. Within the tight-binding approach only a few nearest neighbors are retained, so for example, we obtain

$$\begin{aligned}\epsilon_k = {} & -2t[\cos(k_x a) + \cos(k_y a)] \\ & - 4t_2 \cos(k_x a)\cos(k_y a) \quad \text{[2D NNN]},\end{aligned} \tag{A3}$$

$$\begin{aligned}\epsilon_k = {} & -2t_s[\cos(k_x a) + \cos(k_y a) + \cos(k_z a)] \\ & - 4t_{s2}[\cos(k_x a)\cos(k_y a) + \cos(k_x a)\cos(k_z a) \\ & + \cos(k_y a)\cos(k_z a)] \quad \text{[sc NNN]},\end{aligned} \tag{A4}$$

$$\begin{aligned}\epsilon_k = {} & -8t_b\left[\cos\left(\frac{k_x a}{2}\right)\cos\left(\frac{k_y a}{2}\right)\cos\left(\frac{k_z a}{2}\right)\right] \quad \text{[bcc NNN]} \\ & - 2t_{b2}[\cos(k_x a) + \cos(k_y a) + \cos(k_z a)],\end{aligned} \tag{A5}$$

$$\begin{aligned}\epsilon_k = {} & -4t_f\left[\cos\left(\frac{k_x a}{2}\right)\cos\left(\frac{k_y a}{2}\right) + \cos\left(\frac{k_x a}{2}\right)\cos\left(\frac{k_z a}{2}\right)\right. \\ & \left. + \cos\left(\frac{k_y a}{2}\right)\cos\left(\frac{k_z a}{2}\right)\right] \quad \text{[fcc NNN]} \\ & - 2t_{f2}[\cos(k_x a) + \cos(k_y a) + \cos(k_z a)].\end{aligned} \tag{A6}$$

We repeat here important definitions already mentioned in the text. The distance a is the nearest-neighbor distance in the 2D and simple cubic (sc) cases, and is the length of the cube in the body-centered-cubic (bcc) and face-centered-cubic (fcc) cases; these latter two each contain eight atoms, one at each vertex, along with one in the center (bcc) and six on the face centers (fcc). Also, t, t_s, t_b, and t_f are the nearest-neighbor hopping parameters and t_2, t_{s2}, t_{b2}, and t_{f2} are the next-nearest-neighbor hopping parameters for the 2D square, 3D sc, 3D bcc, and 3D fcc lattices, respectively.

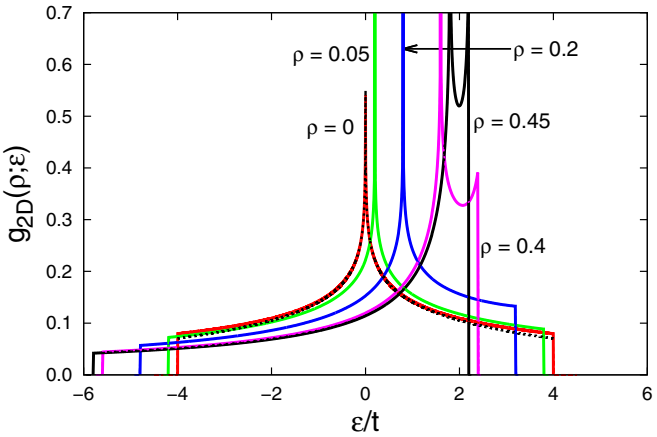

FIG. 13. Plot of the tight-binding 2D density of states for various values of the next-nearest-neighbor (NNN) hopping parameter, $\rho \equiv t_2/t$, as given analytically in Eq. (A7). A logarithmic singularity remains even in the presence of NNN. Note that the results for negative values of ρ are symmetric (about $\epsilon = 0$) to those shown with positive values of ρ. As mentioned in the text, numerical results, using Eq. (A8), are also shown, and are indistinguishable from the analytical results. The black dashed curve is the approximation given by Eq. (15) in the text, valid for $\rho = 0$.

Note that without NNN hopping these have bandwidths W of $8t$, $12t_s$, $16t_b$, and $16t_f$, respectively. We have additionally included next-nearest-neighbor hopping in all these cases; for the 3D cases all but the sc case exhibit singularities when only nearest-neighbor hops are considered; in two dimensions the existence of a singularity is retained as next-nearest-neighbor hops are introduced, while in the three dimensions, in either the face-centered-cubic (fcc) or body-centered-cubic (bcc) cases, the singularity disappears.

For our purposes the important property emerging from these different band dispersions is the shape of the density of states, defined above. In two dimensions, the DOS can be determined analytically in terms of complete elliptic integrals. The result is

$$g_{2\mathrm{D}}(\rho;\epsilon) = \frac{1}{2\pi^2 t a^2}\frac{1}{\sqrt{1-4\rho\bar{\epsilon}}}K\left[1 - \frac{(\rho-\bar{\epsilon})^2}{1-4\rho\bar{\epsilon}}\right], \tag{A7}$$

where $\bar{\epsilon} \equiv \epsilon/(4t)$ and $\rho \equiv t_2/t$, with the restriction that $-1/2 < \rho < 1/2$. A different expression applies for $|\rho| > 1/2$, but we omit this regime as being unphysical. Figure 13 shows the DOS for a few values of $\rho > 0$; note that $g_{2\mathrm{D}}(\rho;\epsilon) = g_{2\mathrm{D}}(-\rho;-\epsilon)$, so the DOS with negative values of ρ are mirror images of those shown. It is evident from Eq. (A7) that the logarithmic singularity occurs at $\epsilon = 4t_2$.

Also shown, but indistinguishable from the analytical curves drawn using Eq. (A7), are results obtained numerically, using the Gaussian representation for a δ function. With $x \equiv k_x a/\pi$ and $y \equiv k_y a/\pi$, the 2D version for the first dispersion

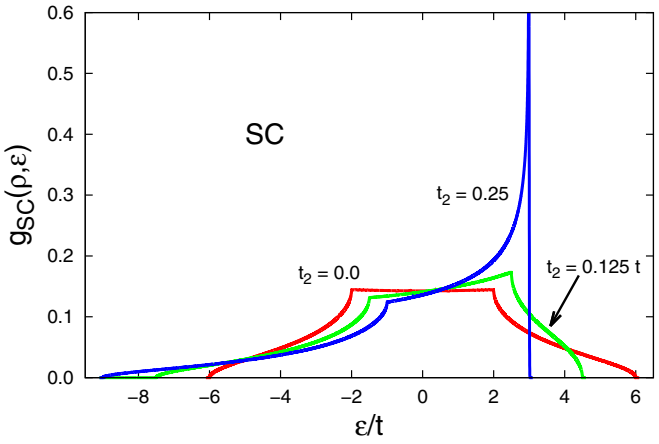

FIG. 14. Plot of the tight-binding 3D SC density of states for various values of the next-nearest-neighbor (NNN) hopping parameter, $\rho \equiv t_2/t$. Note that a singularity develops at the top of the band, for $\epsilon = 3t$, as the two van Hove singularities (originally at $\epsilon = 2t$ and at $\epsilon = 6t$ for $t_2 = 0$) merge into one. Results are shown for positive t_2 since the results for negative values of ρ are symmetric (about $\epsilon = 0$) to those shown with positive values of ρ.

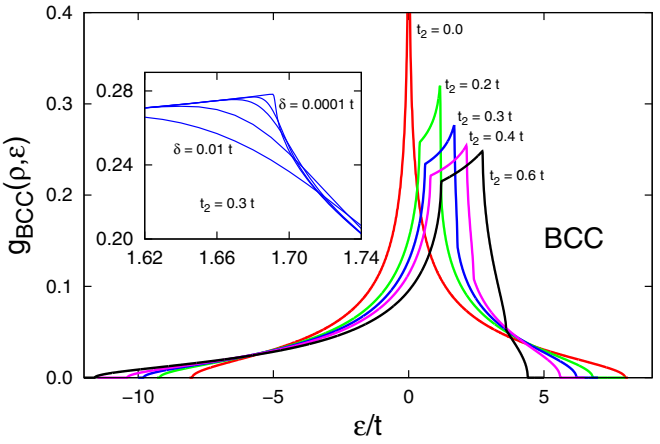

FIG. 15. Plot of the tight-binding 3D bcc density of states for various values of the next-nearest-neighbor (NNN) hopping parameter, $\rho \equiv t_2/t$. Note that the singularity for $\epsilon = 0$ disappears as t_2 becomes nonzero. Results are shown for positive t_2 since the results for negative values of ρ are symmetric (about $\epsilon = 0$) to those shown with positive values of ρ. Even with nonzero t_2 a significant peak in the density of states remains. The inset shows numerical results as a function of ϵ very close to the cusp located at $\epsilon_{\rm cusp} = 6t\rho - 4\rho^3 t$ for $\rho = t_2/t = 0.3$, for various values of the smearing parameter, $\delta/t = 0.01, 0.005, 0.002, 0.001, 0.0001$.

given in Eq. (A6) is

$$g_\delta(\epsilon) = \frac{1}{2ta^2}\frac{1}{\sqrt{\pi\delta^2}}\int_0^1 dx \int_0^1 dy \exp\left\{-\left[\frac{\epsilon - \epsilon_k}{2t\delta}\right]^2\right\}, \tag{A8}$$

where the approximation improves for smaller value of the smearing parameter, δ. In Fig. 13 we use $\delta = 0.0005t$. For 3D dispersions an additional integral over $z \equiv k_z a/\pi$ from zero to unity is required and $a^2 \to a^3$.

In three dimensions, the integrals must be done numerically. It is straightforward to simplify some of the results when there is no next-nearest-neighbor hopping, [17] and we cite some of these results for convenience. For the rest we develop formulas in some instances or simply use Eq. (A8), as this is straightforward and continues to work extremely well, even in three dimensions.

The result for SC with next-nearest-neighbor hopping is

$$g_{\rm SC}(\epsilon) = \int \frac{dx}{2\pi^2 t a^3}\frac{K(y)}{\sqrt{(1+2\rho\cos\pi x)^2 - \rho(4\bar{\epsilon} + 2\cos\pi x)}}, \tag{A9}$$

where

$$y \equiv 1 - \frac{\left(\rho - \bar{\epsilon} - \frac{1}{2}\cos\pi x\right)^2}{(1+2\rho\cos\pi x)^2 - \rho(4\bar{\epsilon} + 2\cos\pi x)} \tag{A10}$$

and $\bar{\epsilon} \equiv \epsilon/(4t)$, $K(y)$ is the complete elliptic integral of the first kind, $\rho \equiv t_2/t$ is the ratio of the NNN to the NN hopping amplitude, and a^3 is the unit cell volume. The limits on the integration are such that y remains positive and less than unity at all times. As remarked in the text, this density of states has no singularities for $t_2 = 0$ [there remain van Hove singularities in the form of cusps and singularities in the derivative of $g(\epsilon)$], but develops a singularity as t_2 increases. This is evident in Fig. 14, where we use the 3D version of Eq. (A8) to plot the density of states.

The result for the bcc lattice with nearest-neighbor hopping only is [17]

$$g_{\rm bcc}(\epsilon) = \frac{2}{a^3}\frac{1}{2\pi^3 t}\int_{|\bar{\epsilon}|}^1 dx \frac{1}{\sqrt{x^2 - \bar{\epsilon}^2}} K[1-x^2]. \tag{A11}$$

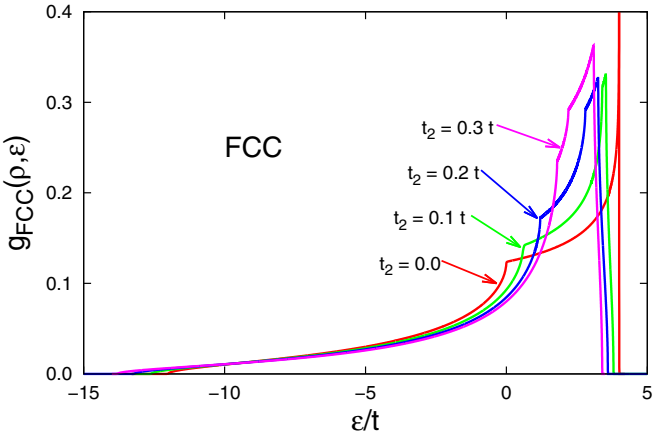

FIG. 16. Plot of the tight-binding 3D fcc density of states for various values of the next-nearest-neighbor (NNN) hopping parameter, $\rho \equiv t_2/t$. For $t_2 = 0$ there is a singularity at the top of the band (red curve as indicated). As t_2 becomes nonzero the singularity disappears and the maximum shifts to the left. In fact, as t_2 grows the maximum in the density of states becomes "robust" in the sense that a significant area exists in the maximum region (also the case with bcc and with the 2D result—see the $\rho = 0.45$ result in Fig. 13).

Note that the unit cell volume for the bcc lattice is $a^3/2$; that is why we isolate this factor at the front of the previous formula. Using the fact that $K(1-x^2) \to \ln(4/x)$ as $x \to 0$, one can straightforwardly derive that

$$\lim_{\bar{\epsilon}\to 0} g_{\rm bcc}(\epsilon) = \frac{2}{a^3}\frac{1}{2\pi^3 t}\left[\frac{3}{2}\ln^2\left(\frac{1}{|\bar{\epsilon}|}\right) + 3\ln 2 \ln\left(\frac{1}{|\bar{\epsilon}|}\right) + 2(\ln 2)^2\right], \quad \text{(A12)}$$

so that the divergence is an $\approx \ln^2(\frac{1}{|\bar{\epsilon}|})$ singularity, stronger than occurs in two dimensions. For the case with NNN hopping we use Eq. (A8) to determine the result numerically; these are shown in Fig. 15. The van Hove points are at energies $-8t - 6t\rho$ (bottom of the band), $2t\rho$, $6t\rho - 4t\rho^3$, $6t\rho$, and $8t - 6t\rho$ (top of the band). Note that the bandwidth remains $16t$ even when NNN hopping is nonzero.

Finally, for fcc, we show numerical results for NNN hopping as well. Our use of the exponential representation of the δ function still allows sufficient resolution to show the various van Hove singularities, apparent in Fig. 16. However, with NNN hopping the singularity at the top of the band for $t_2 = 0$ disappears, but various cusps remain, signifying discontinuities in the first derivative. Note that the fcc lattice is not bipartite, and nesting is not present, even in the case of NN hopping only.

[1] J. Bardeen, L. N. Cooper, and J. R. Schrieffer, Theory of superconductivity, Phys. Rev. **106**, 162 (1957); **108**, 1175 (1957).

[2] J. Labbé. S. Barišić, and J. Friedel, Strong-Coupling Superconductivity in V_3X Type of Compounds, Phys. Rev. Lett. **19**, 1039 (1967).

[3] S. J. Nettel and H. Thomas, Electron-density of states and superconducting T_c in A15-compounds, Solid State Commun. **21**, 683 (1977).

[4] P. Horsch and H. Rietschel, New aspect of superconductivity in A-15 compounds, Z. Phys. B **27**, 153 (1977).

[5] S. G. Lie and J. P. Carbotte, Dependence of T_c on electronic density of states, Solid State Commun. **26**, 511 (1978).

[6] K. M. Ho, M. L. Cohen, and W. E. Pickett, Maximum Superconducting Transition-Temperatures in A15 Compounds, Phys. Rev. Lett. **41**, 815 (1978).

[7] W. E. Pickett, Effect of a varying density of states on superconductivity, Phys. Rev. B **21**, 3897 (1980).

[8] B. Mitrović and J. P. Carbotte, Effects of energy-dependence in the electronic density of states on some normal state properties, Can. J. Phys. **61**, 758 (1983); Effects of energy-dependence in the electronic density of states on some superconducting properties, **61**, 784 (1983); Free-energy formula for a strong coupling superconductor with energy-dependent electronic density of states, **61**, 872 (1983).

[9] See, for example, the very recent review by G. R. Stewart, in Superconductivity in the A15 structure, Physica C **514**, 28 (2015), special issue on superconducting materials, edited by J. E. Hirsch, M. B. Maple, and F. Marsiglio.

[10] J. E. Hirsch and D. J. Scalapino, Enhanced Superconductivity in Quasi Two-dimensional Systems, Phys. Rev. Lett. **56**, 2732 (1986).

[11] J. Labbé and J. Bok, Superconductivity in alcaline-earth-substituted La_2CuO_4: a theoretical model, Europhys. Lett. **3**, 1225 (1987).

[12] C. C. Tsuei, D. M. Newns, C. C. Chi, and P. C. Pattnaik, Anomalous Isotope Effect and van Hove Singularity in Superconducting Cu Oxides, Phys. Rev. Lett. **65**, 2724 (1990).

[13] R. S. Markiewicz, A Survey of the van Hove scenario for high-t_c superconductivity with special emphasis on pseudogaps and striped phases, J. Phys. Chem. Solids **58**, 1179 (1997).

[14] J. Bok and J. Bouvier, Superconductivity and the van Hove scenario, J. Supercond. Nov. Magn. **25**, 657 (2012).

[15] O. K. Andersen, A. I. Liechtenstein, O. Rodriguez, I. I. Mazin, O. Jepsen, V. P. Antropov, O. Gunnarsson, and S. Gopalan, Electrons, phonons, and their interaction in $YBa_2Cu_3O_7$, Physica C **185-189**, 147 (1991).

[16] A. A. Abrikosov, J. C. Campuzano, and K. Gofron, Experimentally observed extended saddle point singularity in the energy spectrum of $YBa_2Cu_3O_{6.9}$ and $YBa_2Cu_4O_8$ and some of the consequences, Physica C **214**, 73 (1993).

[17] R. J. Jelitto, The density of states of some simple excitations in solids, J. Phys. Chem. Solids **30**, 609 (1969).

[18] D. Duan, Y. Liu, F. Tian, D. Li, X. Huang, Z. Zhao, H. Yu, B. Liu, W. Tian, and T. Cui, Pressure-induced metallization of dense $(H_2S)_2H_2$ with high-T_c superconductivity, Sci. Rep. **4**, 6968 (2014).

[19] N. Bernstein, C. Stephen Hellberg, M. D. Johannes, I. I. Mazin, and M. J. Mehl, What superconducts in sulfur hydrides under pressure and why, Phys. Rev. B **91**, 060511(R) (2015).

[20] A. P. Drozdov, M. I. Eremets, I. A. Troyan, V. Ksenofontov, and S. I. Shylin, Conventional superconductivity at 203 kelvin at high pressures in the sulfur hydride system, Nature (London) **525**, 73 (2015).

[21] We became aware of Ref. [28] recently; they have investigated retardation effects and indeed find that a reduction in T_c will occur as a result of their inclusion.

[22] P. Nozières and S. Schmitt-Rink, Bose condensation in an attractive Fermion gas—from weak to strong coupling superconductivity, J. Low Temp. Phys. **59**, 195 (1985).

[23] A recent description of the two-dimensional electron gas with attractive interactions within the T-matrix formalism is given in F. Marsiglio, P. Pieri, A. Perali, F. Palestini, and G. C. Strinati, Pairing effects in the normal phase of a two-dimensional Fermi gas, Phys. Rev. B **91**, 054509 (2015).

[24] F. Marsiglio, Eliashberg theory of the critical temperature and isotope effect. Dependence on bandwidth, band-filling, and direct Coulomb repulsion, J. Low Temp. Phys. **87**, 659 (1992).

[25] F. Marsiglio and J. P. Carbotte, Electron-Phonon Superconductivity, Review Chapter in *Superconductivity, Conventional and Unconventional Superconductors*, edited by K. H.

Bennemann and J. B. Ketterson (Springer-Verlag, Berlin, 2008), pp. 73–162.

[26] G. M. Eliashberg, Interactions between electrons and lattice vibrations in a superconductor, Zh. Eksp. Teor. Fiz. **38**, 966 (1960) [Sov. Phys. JETP **11**, 696 (1960)].

[27] Y. Quan and W. E. Pickett, van Hove singularities and spectral smearing in high-temperature superconducting H_3S, Phys. Rev. B **93**, 104526 (2016).

[28] W. Sano, T. Koretsune, T. Tadano, R. Akashi, and R. Arita, Effect of van Hove singularities on high-T_c superconductivity in H_3S, Phys. Rev. B **93**, 094525 (2016).

[29] J. R. Schrieffer, *Theory of Superconductivity* (Benjamin/Cummings, Don Mills, 1964).

[30] M. Tinkham, *Introduction to Superconductivity*, 2nd ed. (McGraw-Hill, New York, 1996).

[31] In this manner retardation effects are taken into account in BCS theory in a very phenomenological way through the imposed cutoff. This cutoff is imposed in momentum space (not in frequency space); nonetheless, use of a simple identity for the factor $1–2f(E_k)$ allows the right-hand side of the so-called gap equation [Eq. (2)] to be rewritten in terms of Matsubara frequencies with a cutoff in this space, so it better resembles Eliashberg theory.

[32] F. W. J. Olver, D. W. Lozier, R. F. Boisvert, and C. W. Clark, *NIST Handbook of Mathematical Functions* (Cambridge University Press, Cambridge, UK, 2010).

[33] One of us (F.M.) has repeatedly asked colleagues in the superconducting community around the world about this for the past 20 years, and with one exception they were not aware of the divergences in three dimensions. The Jelitto paper [17] has been cited more than 140 times, so clearly some researchers are aware of this fact. However, neither of Refs. [18,19] cite the Jelitto paper. While later references [27,34] cite a van Hove singularity, neither of these seem to be aware that the relevant van Hove singularity is likely a remnant of the BCC singularity (when only NN hopping is included). Reference [35] actually uses a rather sophisticated tight-binding model to achieve a good fit with first-principle calculations, but they also appear to be unaware of the BCC singularity lurking nearby in parameter space.

[34] D. A. Papaconstantopoulos, B. M. Klein, M. J. Mehl, and W. E. Pickett, Cubic H_3S around 200 GPa: An atomic hydrogen superconductor stabilized by sulfur, Phys. Rev. B **91**, 184511 (2015).

[35] L. Ortenzi, E. Cappelluti, and L. Pietronero, Band structure and electron-phonon coupling in H_3S: A tight-binding model, Phys. Rev. B **94**, 064507 (2016).

[36] F. Marsiglio, Pairing and charge-density-wave correlations in the Holstein model at half-filling, Phys. Rev. B **42**, 2416 (1990).

[37] J. M. Kosterlitz and D. J. Thouless, Ordering, metastability and phase-transitions in 2-dimensional systems, J. Phys. C **6**, 1181 (1973).